Journal of Theoretical and Applied Mechanics, Sofia, Vol.54 (2024) pp. 339-355
FLUID MECHANICS

NUMERICAL STUDY OF 2D STEADY FLUID FLOW IN LID-DRIVEN RECTANGULAR DOMAIN WITH TEMPERATURE EFFECT USING HYBRID FINITE VOLUME METHOD

V. AMBETHKAR, JYOTI*

Department of Mathematics, Faculty of Mathematical Sciences, University of Delhi, Delhi-110007, India

[Received: 22 November 2023. Accepted: 1 October 2024]

doi: https://doi.org/10.55787/jtams.24.54.3.339

ABSTRACT: This paper investigates the numerical simulation for the two dimensional (2D) steady fluid flow by using hybrid finite volume method in the lid-driven rectangular domain. The top wall is moving with a constant speed in the positive horizontal direction and other walls are in rest. Different constant temperature are applied to the top and bottom wall and left and right walls are thermally insulated. The dimensionless governing equations are discritized using the hybrid scheme of finite volume method. The SIMPLE algorithm is used to compute the numerical solution of the flow variables such as u-velocity, v-velocity, pressure (p) and temperature (θ). u-velocity is maximum on the top wall and it is decreasing as we go down till the geometric center. v-velocity is maximum near the top left corner and minimum near the top right corner of the domain. Pressure contour graph shows the maximum pressure near the top right corner and minimum near top left corner. Temperature contour graph shows the maximum temperature on the bottom wall and it will decrease as we goes towards the top wall.

KEY WORDS: Finite volume method, staggered grid, lid-driven flow, hybrid scheme, numerical discretization.

1 INTRODUCTION

The present problem of investigates the numerical simulation for the two dimensional (2D) steady fluid flow by using hybrid finite volume method in the lid-driven rectangular domain is important due to its numerous applications. Fluid flow problems are prevalent in various engineering and scientific fields, ranging from the design of efficient pipelines and heat exchangers to simulating natural phenomena like weather patterns and groundwater flow. The Finite Volume Method (FVM) divides the computational domain into discrete control volumes and conservatively represents the

*Corresponding author e-mail: jkaushik@maths.du.ac.in

conservation equations of mass, momentum, and energy within these volumes. While FVM itself is a robust and versatile approach, the hybrid scheme enhances its capabilities by combining it with other numerical methods to address specific challenges and optimize computational efficiency. This introduction immerse into the finite volume method with a focus on its hybrid scheme, an advanced technique that merges the strengths of the FVM with other numerical methods. It provides a powerful tool to address complex geometries, non-linearities, and discontinuities in fluid flow simulations, making it an invaluable tool for engineers and scientists seeking accurate and efficient solutions.

Ambethkar, Basumatary [1], Piller, Stalio [2], Bruneau, Jouron [3] and Erturk et al. [4] have investigated on implementation of the finite volume scheme(FVM) based on staggered grid for solving the partial differential equations which are the governing equation for ow with heat transfer in square and rectangular region. Ghia et al. [5] have validated their approach through numerical experiments and comparisons with benchmark solutions, demonstrating the accuracy and efficiency of their method which we used to check our results and found them extremely accurate.

Salem [6] discusses numerical methods for solving the incompressible Navier-Stokes equations, which describe the behavior of fluid flow and primitive variables used that include velocity components and pressure, which are primary variables in the incompressible flow formulation. Corcione [7] investigates the heat transfer characteristics of nanofluids within rectangular enclosures under the influence of buoyancy forces, with one set of sidewalls being differentially heated and they suggest potential applications or future research directions related to buoyancy-driven nanofluid heat transfer. Animasaun et al. [8] have provided the theoretical framework for understanding the relationship between momentum diffusivity and thermal diffusivity that involve mathematical models and equations. Kuznetsov, Sheremet [9] provide details of the numerical method they employ to solve the Navier-Stokes equations for high Reynolds number flows. In this case, they mention the use of a multigrid method, which is a technique for solving partial differential equations efficiently. Kalita et al. [10] have provided discussion on the grid resolution that is crucial in computational fluid dynamics. The paper addresses the grid refinement strategy used to ensure accurate results for higher-order computation.

Motivation for this study is due to enormous applications of study of 2D flow in lid-Driven rectangular domain. This paper aims to investigate the numerical simulation for the two dimensional (2D) steady fluid flow by using hybrid finite volume method in the lid-driven rectangular domain.

The summary of this paper comprises of mathematical formulation in Section 2 which includes the geometry of the problem and non-dimensional governing equation. Numerical discretization is given in Section 3. In Section 4 stability, numerical

convergence and code validation are discussed. In Section 5 result and discussion; and conclusions are discussed in Section 6.

2 Mathematical Formulation

2.1 Geometrical description of the problem

Figure 1 shows the geometry of the problem considered in this work along with the boundary conditions. A lid-driven rectangular cavity around the point (1.0,0.5) in which laminar steady incompressible flow is considered. The upper(top) wall is moving with constant speed of 1 m/s in the positive x-direction and other walls of the domain are in rest. The horizontal walls are maintainted at different constant tempra-ture $\theta = 0^\circ$ and $\theta = 1^\circ$. The top wall considered as cold wall and the bottom wall as hot wall. The vertical walls are adiabatic.

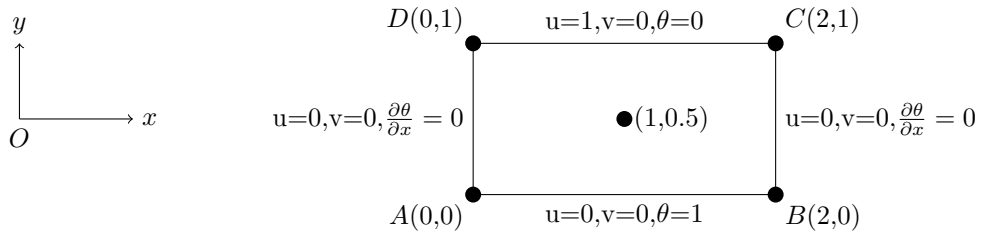

Fig. 1: Geometry of the problem.

The boundary conditions are set as follows:

$$\begin{aligned}
&\text{on plate } AB: \quad u = 0; \quad v = 0; \quad \theta = 1\\
&\text{on plate } DC: \quad u = 1; \quad v = 0; \quad \theta = 0\\
&\text{on plate } AD: \quad u = 0; \quad v = 0; \quad \partial\theta/\partial x = 0\\
&\text{on plate } BC: \quad u = 0; \quad v = 0; \quad \partial\theta/\partial x = 0
\end{aligned}$$

where AB, BC, CD, DA are the bottom, right, top and left walls of the four-sided rectangular region.

2.2 Governing equations

The governing equations for the problem under consideration are based on two-dimensional continuity equation, linear momentum in x and y direction. The flow is assumed to be steady and incompressible. The governing equations under the prior assumptions can be expressed in non-dimensional form as follows:

(1) continuity equation: $$\frac{\partial u}{\partial x} + \frac{\partial v}{\partial y} = 0\,,$$

$$\text{(2)}\quad x\text{-momentum equation:}\quad u\frac{\partial u}{\partial x}+v\frac{\partial u}{\partial y}=-\frac{\partial p}{\partial x}+\frac{1}{Re}\Big(\frac{\partial^2 u}{\partial x^2}+\frac{\partial^2 u}{\partial y^2}\Big),$$

$$\text{(3)}\quad y\text{-momentum equation:}\quad u\frac{\partial v}{\partial x}+v\frac{\partial v}{\partial y}=-\frac{\partial p}{\partial y}+\frac{1}{Re}\Big(\frac{\partial^2 v}{\partial x^2}+\frac{\partial^2 v}{\partial y^2}\Big)+Ra\,Pr\,\theta,$$

$$\text{(4)}\quad \text{energy equation:}\quad u\frac{\partial \theta}{\partial x}+v\frac{\partial \theta}{\partial y}=\frac{1}{Re\,Pr}\Big(\frac{\partial^2 \theta}{\partial x^2}+\frac{\partial^2 \theta}{\partial y^2}\Big),$$

where u, v, θ, p, are the dimensionless velocity components in x and y directions, dimensionless temperature, dimensionless pressure. Reynolds number is defined by $Re = \rho u L/\mu$, Rayleigh number is defined by $Ra = g\beta(\theta - \theta_\infty)L^3/\nu_\alpha$, and the Prandtl number is defined by $Pr = \nu/\alpha$, where ρ is the density, L is the characteristic length, μ is the dynamic viscosity of the fluid, g is the acceleration due to gravity, β is the coefficient of thermal expansion, θ is the surface temperature, θ_∞ is the bulk temperature, ν is the kinematic viscosity, α is the thermal diffusivity.

3 Numerical Discretization

The hybrid finite volume scheme is used to compute the numerical solutions of lid-driven rectangular cavity. The hybrid scheme combines two other common interpolation schemes upwind and central differencing scheme. It provides a balance between accuracy and stability for the Navier-Stokes equation. The order of approximation for the convective term can be second-order for low convection ($Pe > 2$) and first-order for high convection ($Pe \leq 2$), while the diffusion term remains second-order. The non-dimensional cell Peclet number as a measure of the relative strengths of convection and diffusion as $Pe = F/D = \rho u \delta x/\Gamma$. The FVM divides the computational domain into discrete control volumes and conservatively represents the conservation equations of mass, momentum, and energy within these volumes. The governing equation of our problem under consideration are discretized on a staggered grid system. In Fig. 2 horizontal and vertical arrows represents the locations where x and y components of velocities are determined. Further the ($\bullet$) location represents the position where the pressure and the temperature are determined. The control volumes around ($\rightarrow$), ($\uparrow$) and ($\bullet$) are the location where we discretized equations for x-momentum, y-momentum and energy (continuity) equation respectively.

In the staggered grid system the discretised u-momentum equation for the velocity at location (i, J) is given by

$$\text{(5)}\qquad a_{i,J}u_{i,J} = \sum a_{nb}u_{nb} + (p_{I-1,J} - p_{I,J})A_{i,J} + b_{i,J}\,,$$

where $A_{i,J}$ is the area and neighbours of $a_{nb}u_{nb}$ are $(i+1, J)$, $(i-1, J)$, $(i, J+1)$ and $(i, J-1)$. The coefficients of hybrid difference scheme along with fluxes and

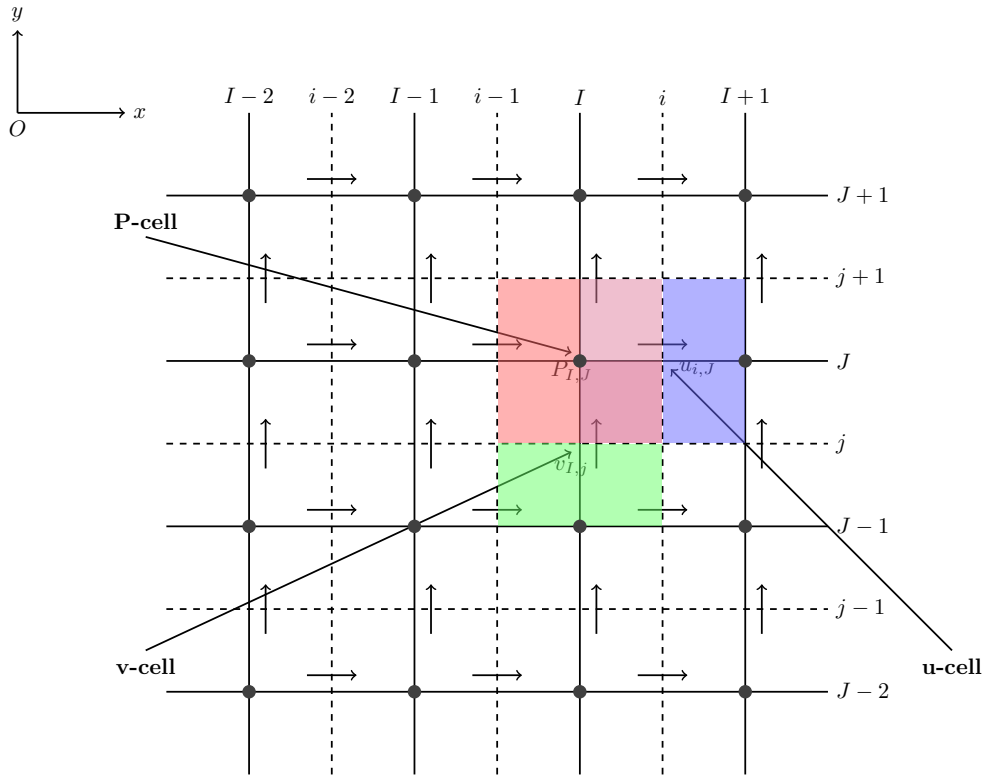

Fig. 2: Staggered grid.

conductance at cell faces of the u-control volume are computed as given in [11] (pp. 197-199)

$$a_{i,J} = a_{i-1,J} + a_{i+1,J} + a_{i,J+1} + a_{i,J-1} + \Delta F\,, \tag{6}$$

where

$$a_{i-1,J} = D_{I-1,J} + \max(F_{I-1,J}, 0), \qquad a_{i+1,J} = D_{I,J} + \max(-F_{I,J}, 0)\,,$$
$$a_{i,J+1} = D_{i,j+1} + \max(-F_{i,j+1}, 0), \qquad a_{i,J-1} = D_{i,j} + \max(F_{i,j}, 0)\,,$$
$$\Delta F = (F_e - F_w) + (F_n - F_s) = (F_{I,J} - F_{I\_1,J}) + (F_{i,j+1} - F_{i,j})$$

and

$$
\begin{aligned}
F_e &= F_{I,J} = \frac{F_{i+1,J} + F_{i,J}}{2} = \frac{u_{i+1,J}A_{i+1,J} + u_{i,J}A_{i,J}}{2}\,,\\
F_w &= F_{I-1,J} = \frac{F_{i,J} + F_{i-1,J}}{2} = \frac{u_{i,J}A_{i,J} + u_{i-1,J}A_{i-1,J}}{2}\,,\\
F_n &= F_{i,j+1} = \frac{F_{I,j+1} + F_{I-1,j+1}}{2} = \frac{v_{I,j+1}A_{I,j+1} + v_{I-1,j+1}A_{I-1,j+1}}{2}\,,\\
F_s &= F_{i,j} = \frac{F_{I,j} + F_{I-1,j}}{2} = \frac{v_{I,j}A_{I,j} + v_{I-1,j}A_{I-1,j}}{2}\,,\\
D_e &= D_{I,J} = \frac{A_{I,J}}{Re\Delta x} = \frac{1}{Re\Delta x}\Big(\frac{A_{i+1,J} + A_{i,J}}{2}\Big),\\
D_w &= D_{I-1,J} = \frac{A_{I-1,J}}{Re\Delta x} = \frac{1}{Re\Delta x}\Big(\frac{A_{i,J} + A_{i-1,J}}{2}\Big),\\
D_n &= D_{i,j+1} = \frac{A_{i,j+1}}{Re\Delta y} = \frac{1}{Re\Delta y}\Big(\frac{A_{I,j+1} + A_{I-1,j+1}}{2}\Big),\\
D_s &= D_{i,j} = \frac{A_{i,j}}{Re\Delta y} = \frac{1}{Re\Delta y}\Big(\frac{A_{I,j} + A_{I-1,j}}{2}\Big).
\end{aligned}
\tag{7}
$$

Similarly, the discretised v-momentum equation for the velocity at location (I, j) is given by

$$
a_{I,j}v_{I,j} = \sum a_{nb}v_{nb} + (p_{I,J-1} - p_{I,J})A_{I,j} + b_{I,j}\,, \tag{8}
$$

where $A_{i,J}$ is the area and neighbours of $a_{nb}v_{nb}$ are $(I+1, j)$, $(I-1, j)$, $(I, j+1)$ and $(I, j-1)$. The coefficients of hybrid differencing scheme are computed as given in [12] (p.122)

$$
a_{I,j} = a_{I-1,j} + a_{I+1,j} + a_{I,j+1} + a_{I,j-1} + \Delta F\,, \tag{9}
$$

where

$$
\begin{aligned}
a_{I-1,j} &= D_{i,j} + \max(F_{i,j}, 0), \qquad a_{I+1,j} = D_{i+1,j} + \max(-F_{i+1,j}, 0)\,,\\
a_{I,j+1} &= D_{I,J} + \max(-F_{I,J}, 0), \qquad a_{I,j-1} = D_{I,J-1} + \max(F_{I,J-1}, 0)\,,\\
\Delta F &= (F_e - F_w) + (F_n - F_s) = (F_{i+1,j} - F_{i,j}) + (F_{I,J} - F_{I,J-1})
\end{aligned}
$$

and

$$
\begin{aligned}
F_e &= F_{i+1,j} = \frac{F_{i+1,J} + F_{i+1,J-1}}{2} = \frac{u_{i+1,J}A_{i+1,J} + u_{i+1,J-1}A_{i+1,J-1}}{2}\,,\\
F_w &= F_{i,j} = \frac{F_{i,J} + F_{i,J-1}}{2} = \frac{u_{i,J}A_{i,J} + u_{i,J-1}A_{i,J-1}}{2}\,,\\
F_n &= F_{I,J} = \frac{F_{I,j+1} + F_{I,j}}{2} = \frac{v_{I,j+1}A_{I,j+1} + v_{I,j}A_{I,j}}{2}\,,\\
F_s &= F_{I,J-1} = \frac{F_{I,j} + F_{I,j-1}}{2} = \frac{v_{I,j}A_{I,j+1} + v_{I,j-1}A_{I,j-1}}{2}\,,\\
D_e &= D_{i+1,j} = \frac{A_{i+1,j}}{Re\Delta x} = \frac{1}{Re\Delta x}\Big(\frac{A_{I+1,J} + A_{I,J}}{2}\Big),\\
D_w &= D_{i,j} = \frac{A_{i,j}}{Re\Delta x} = \frac{1}{Re\Delta x}\Big(\frac{A_{I,j} + A_{I-1,j}}{2}\Big),\\
D_n &= D_{I,J} = \frac{A_{I,J}}{Re\Delta y} = \frac{1}{Re\Delta y}\Big(\frac{A_{i+1,J} + A_{i,J}}{2}\Big),\\
D_s &= D_{I,J-1} = \frac{A_{I,J-1}}{Re\Delta y} = \frac{1}{Re\Delta y}\Big(\frac{A_{i+1,J-1} + A_{i,J-1}}{2}\Big).
\end{aligned}
\tag{10}
$$

and the pressure correction equation obtained from continuity equation

$$
a_{I,J}p'_{I,J} = \sum a_{nb}p'_{nb} + b'_{I,J}\,,
\tag{11}
$$

where

$$
a_{I,J} = a_{I+1,J} + a_{I-1,J} + a_{I,J+1} + a_{I,J-1}
$$

and the coefficients are

$$
\begin{aligned}
a_{I+1,J} &= (dA)_{i+1,J}\,, \qquad a_{I-1,J} = (dA)_{i,J}\,,\\
a_{I,J+1} &= (dA)_{I,j+1}\,, \qquad a_{I,J-1} = (dA)_{I,j-1}\,,\\
d_{i,J} &= \frac{A_{i,J}}{a_{i,J}}\,, \qquad d_{I,j} = \frac{A_{I,j}}{a_{I,j}}\,,\\
b'_{I,J} &= (u^*A)_{i,J} - (u^*A)_{i+1,J} + (v^*A)_{I,j} - (v^*A)_{I,j+1}\,.
\end{aligned}
\tag{12}
$$

The equation (11) represents the discretized continuity equation evaluated in terms of pressure correction p'. The source term b' in this equation is continuity inbalance equation arising from the incorrect velocity field u^* and v^*. By solving equation (12), the pressure correction field p' is obtained at all points.

4 NUMERICAL SCHEME

4.1 STABILITY AND CONVERGENCE OF THE NUMERICAL SCHEME

Numerical calculations are performed to obtain the solutions of the flow variables. The dimensionless parameters such as *Pr*, *Re* and *Ra* are choosen appropriately. The solution obtained from the FVM schemes are based on the iterative method. Hence these iterative solutions are always convergent. Moreover the validation of these results are done and are given in Fig. 4 and Fig. 5. Here SIMPLE algorithm is used to calculate the solutions of the flow variables which is given below.

SIMPLE ALGORITHM

- Guess velocity and pressure fields u^*, v^* and p^*
- Solve the discretised momentum equations
- Obtained converged u^*, v^* and p^*. Calculate b term of pressure-correction equation
- Solve the pressure correction equation to converge
- Correct u, v and p using

$$u_{i,J} = u^*_{i,J} + d_{i,J}(p'_{I-1,J} - p'_{I,J})$$
$$v_{I,j} = u^*_{I,j} + d_{I,j}(p'_{I,J-1} - p'_{I,J})$$
$$p = p^* + p'$$

- Solve for θ
- Check for convergence

The convergence is justified from the flow chart given in Fig. 3

4.2 CODE VALIDATION

This paper numerically investigates the flow in rectangular lid-driven cavity heated at the bottom wall. The top and bottom walls have a consistent mass distribution. The adiabatic top and bottom walls obstruct mass transmission. The numerical solutions to the problem under investigation are computed using MATLAB code, which is written and executed. We compared our flow findings to those available in the literature and found them extremely accurate in evaluating our MATLAB code. Here

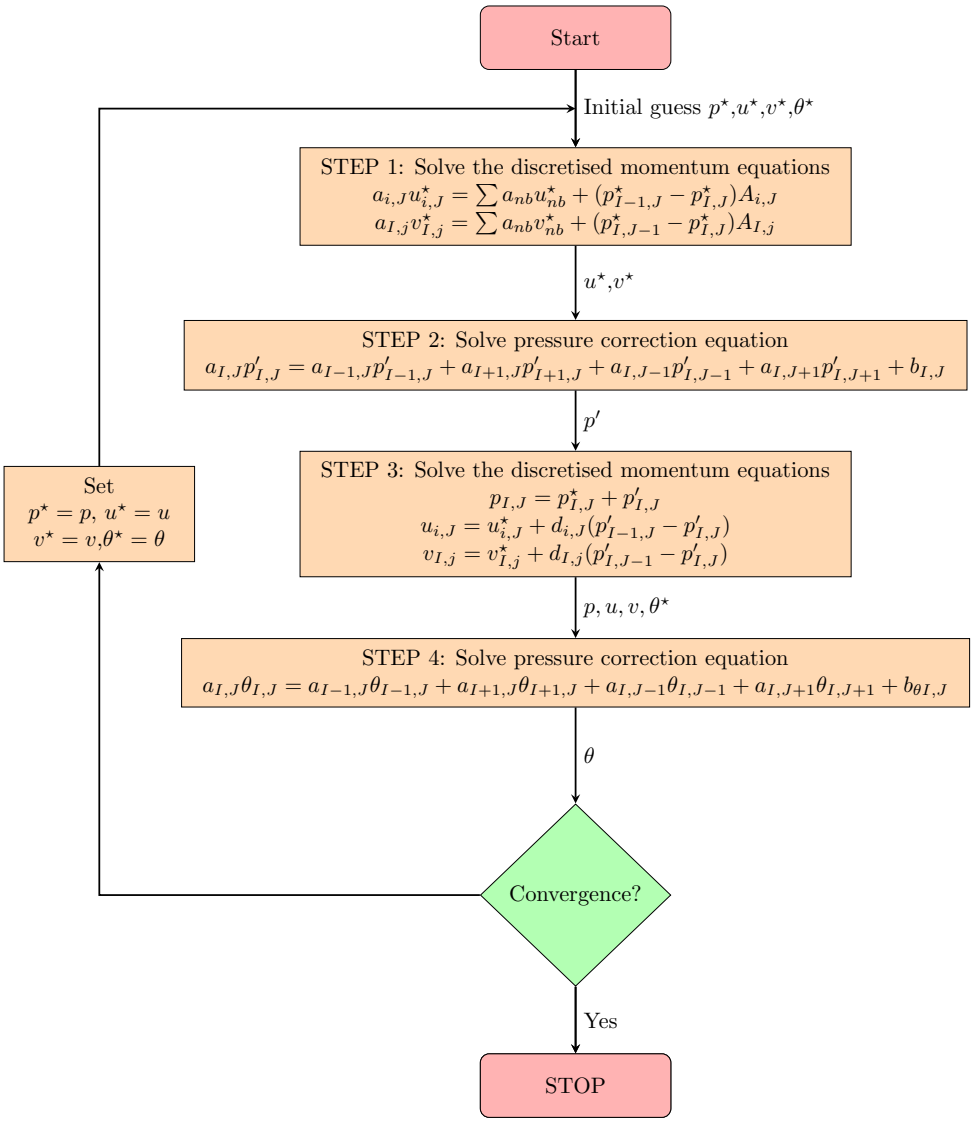

Fig. 3: SIMPLE algorithm flow chart.

we compared the Ghia's steady state and present result for the lid-driven square cavity flow u-velocity from bottom to top wall through geometric center and v-velocity from left to right wall through geometric center as shown in Fig. 4 and Fig. 5, where we found good agreement.

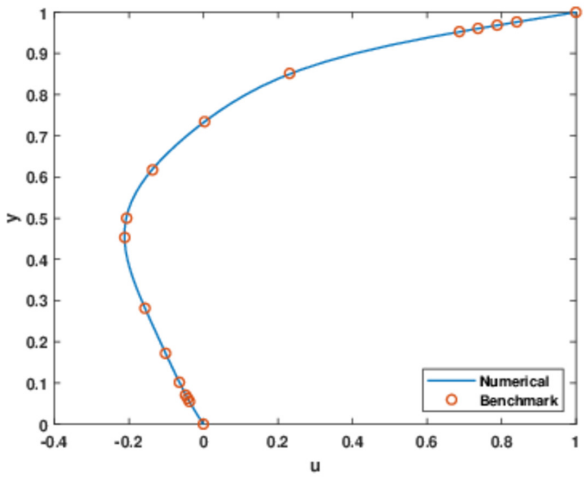

Fig. 4: Comparison of Ghia's steady state and present result for the lid-driven square cavity flow u-velocity from bottom to top wall through geometric center for $Pr = 0.7$, $Re = 100$ and $Ra = 100$.

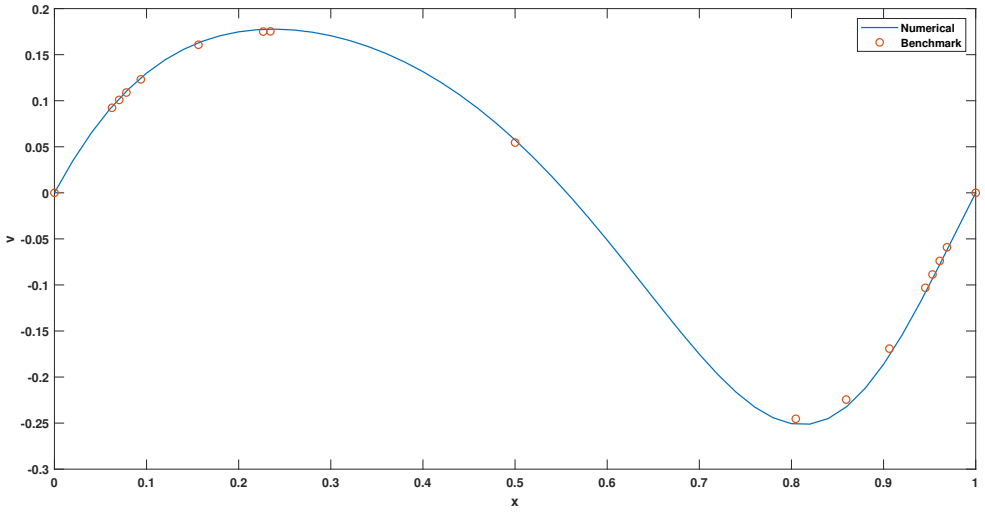

Fig. 5: Comparison of Ghia's steady state and present result for the lid-driven square cavity flow v-velocity from left to right wall through geometric center for $Pr = 0.7$, $Re = 100$ and $Ra = 100$.

5 Results and Discussion

The current study investigates the ow variables and temperature distribution of a lid-driven rectangular cavity. Figure 6 represents the graph of residual error vs. number of iteration. This graph gives the information how many iterations are required to obtain the error of order 10^{-7}. The variation of u-velocity decreases from the bottom wall until the geometric center and then increases till the top wall of the rectangular domain as shown in Fig. 7. The variation of the v-velocity increases from the left wall until the geometric center and then decreases in the rectangular domain as shown in Fig. 8. The u-velocity is maximum on the top wall and it is decreasing as we go down till the geometric center. The v-velocity is maximum near the top left corner and minimum near the top right corner of the domain. Figures 9 and 10 describe an information about the behviour of u-velocity from left to right wall and v-velocity from bottom to top wall through the geometric center. The contour plots of velocity are shown in the Figs. 11 and 12 give the information of u-velocity and v-velocity within the rectangular domain. The colorbar gives the information of the magnitude of the velocity. In Fig. 13 pressure contour graph shows that the maximum pressure near the top right corner and minimum near top left corner. Temperature contour

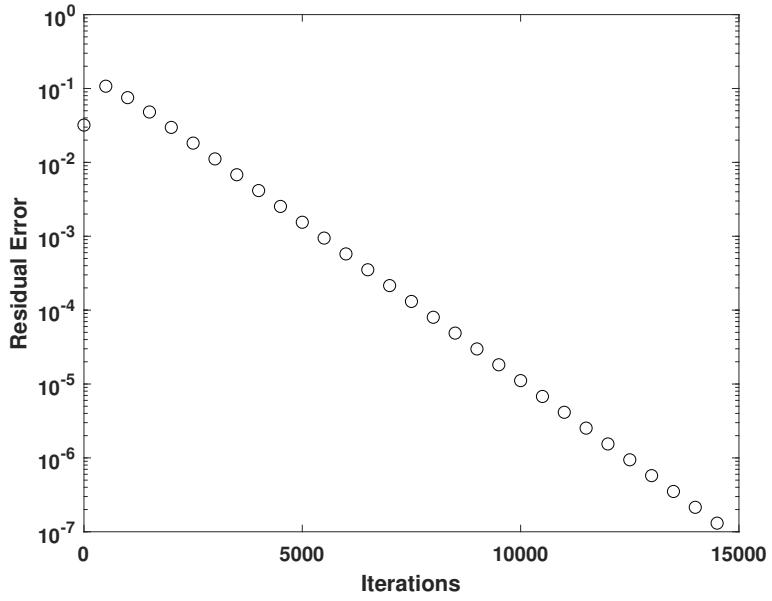

Fig. 6: Residual error occurs in the SIMPLE algorithm using hybrid scheme for $Pr = 0.7$, $Re = 100$ and $Ra = 100$.

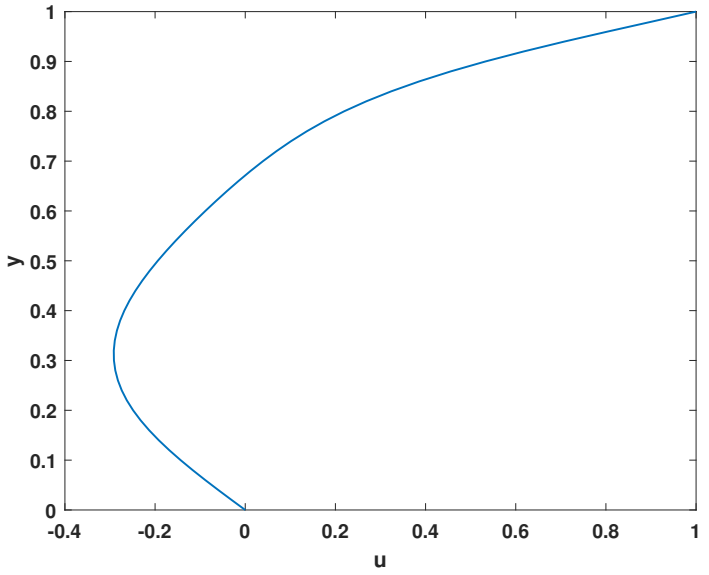

Fig. 7: Behaviour of u-velocity from bottom to top wall through the geometric center for $Pr = 0.7$, $Re = 100$ and $Ra = 100$.

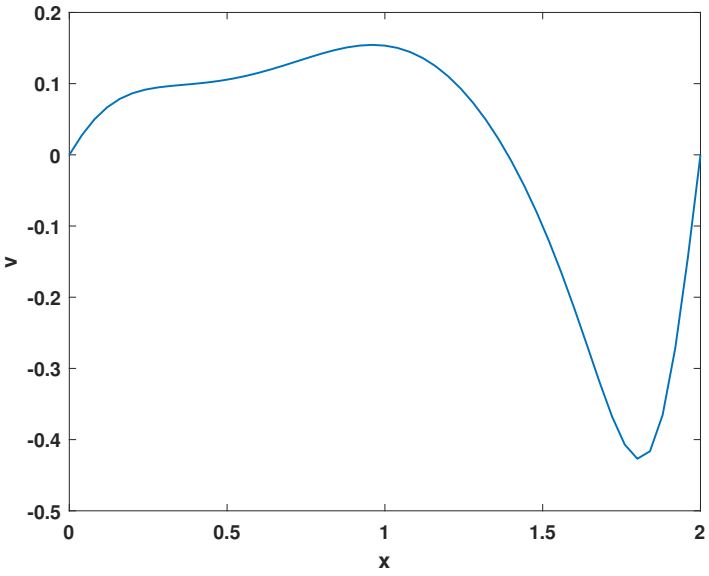

Fig. 8: Behaviour of v-velocity from left to right wall through the geometric center for $Pr = 0.7$, $Re = 100$ and $Ra = 100$.

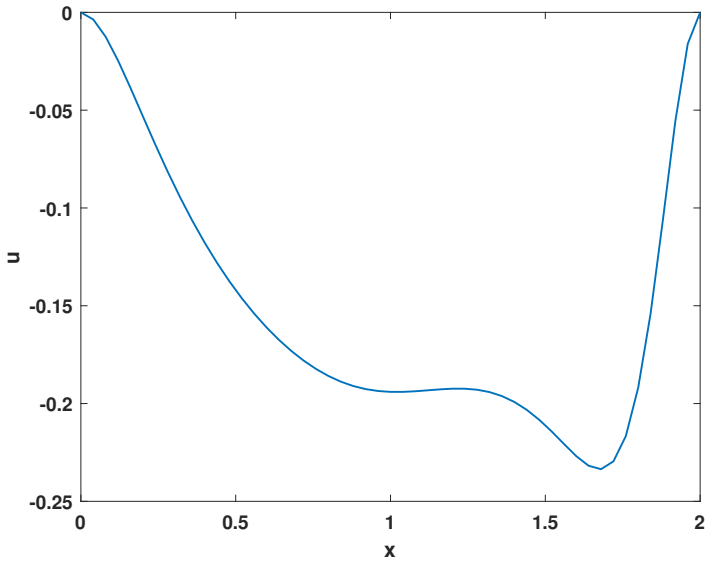

Fig. 9: Behaviour of u-velocity from left to right wall through the geometric center for $Pr = 0.7$, $Re = 100$ and $Ra = 100$.

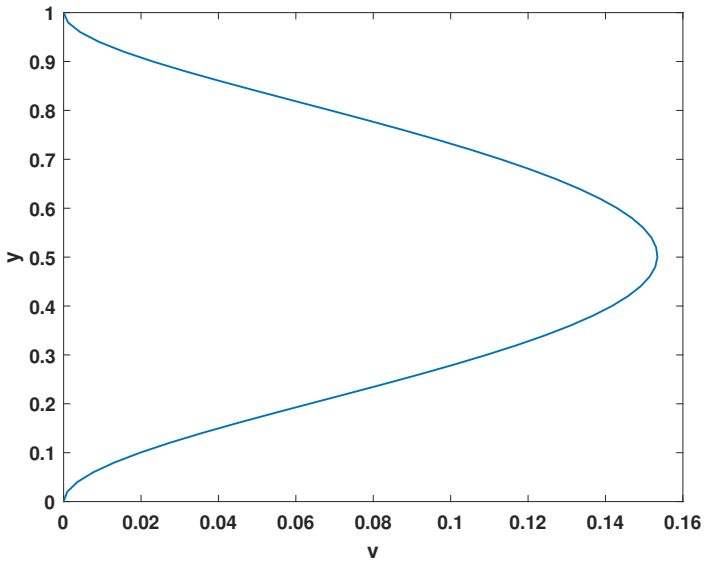

Fig. 10: Behaviour of v-velocity from bottom to top wall through the geometric center for $Pr = 0.7$, $Re = 100$ and $Ra = 100$.

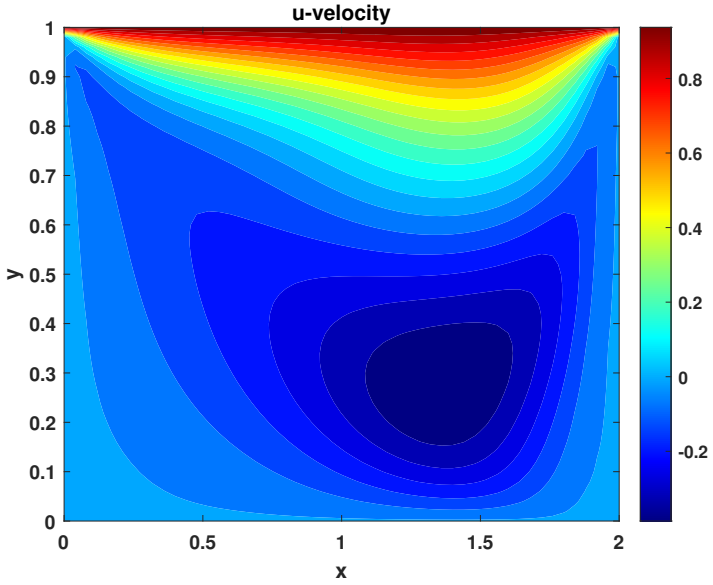

Fig. 11: u-velocity contour graph for $Pr = 0.7$, $Re = 100$ and $Ra = 100$.

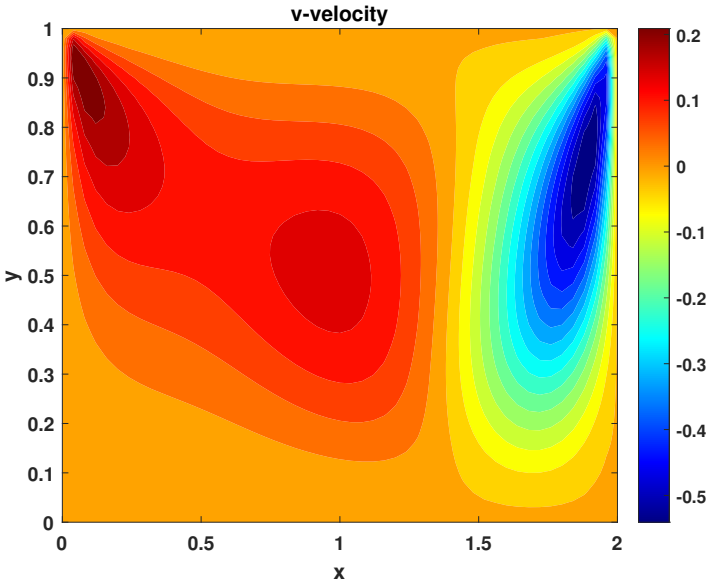

Fig. 12: v-velocity contour graph for $Pr = 0.7$, $Re = 100$ and $Ra = 100$.

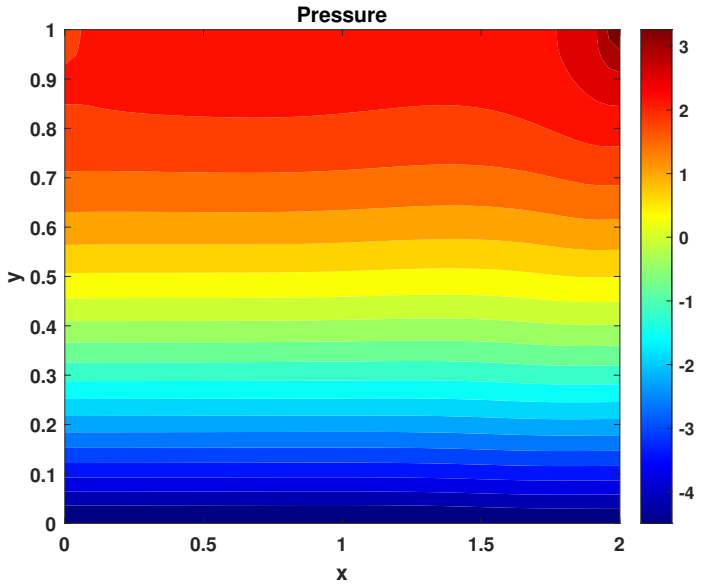

Fig. 13: Pressure contour graph for $Pr = 0.7$, $Re = 100$ and $Ra = 100$.

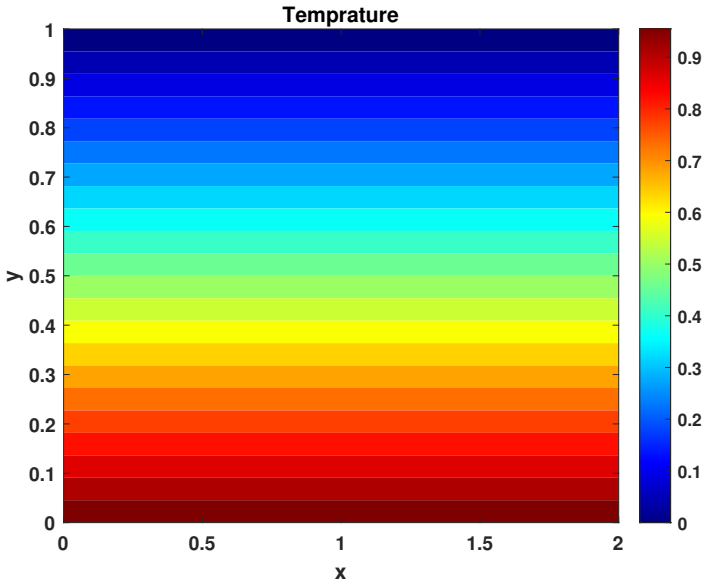

Fig. 14: Temperature contour graph for $Pr = 0.7$, $Re = 100$ and $Ra = 100$.

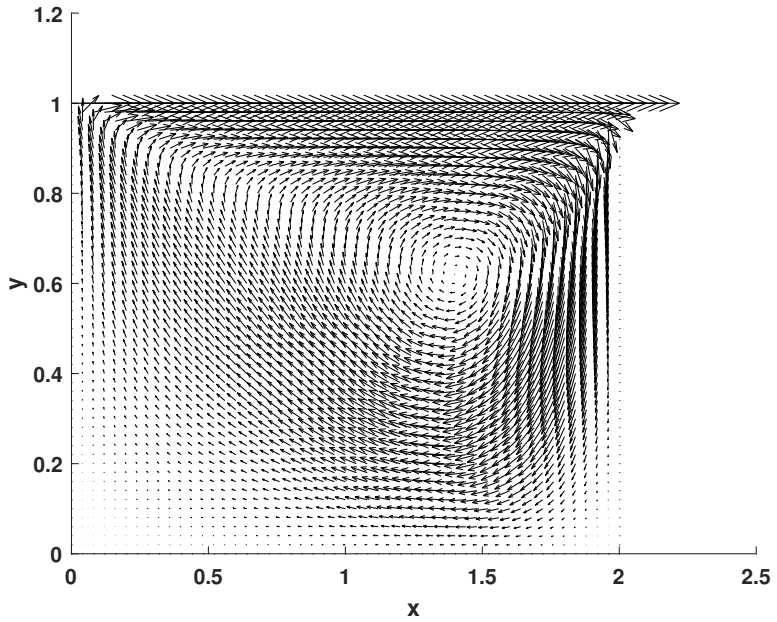

Fig. 15: u-, v-velocity behaviour in the rectangular cavity for $Pr = 0.7$, $Re = 100$ and $Ra = 100$.

graph shows the maximum temperature on the bottom wall and it will decrease as we go towards the top wall as shown in Fig. 14. In Fig. 15 vector field plot shows the flow field in the rectangular lid-driven cavity.

6 Conclusions

The current study investigates the flow and temperature distribution of a lid-driven rectangular cavity. The variation of u-velocity, v-velocity from bottom wall to top wall and from left wall to right wall through the geometric center of the rectangular domain. u-velocity is maximum on the top wall and it is decreasing as we go down till the geometric center. v-velocity is maximum near the top left corner and minimum near the top right corner of the domain. Pressure contour graph shows the maximum pressure near the top right corner and minimum near top left corner. Temperature contour graph shows the maximum temperature on bottom wall and it will decrease as we go towards the top wall. Vector field plot shows the flow field in the rectangular lid-driven cavity.

ACKNOWLEDGMENT

The first author acknowledges the financial support received from the DST-SERB Project No. EEQ/2022/001081 dated 20th January 2023. The second author acknowledges Grants Commission, New Delhi, for providing financial support vide letter number Ref. No. 1055/CSIR-UGC NET JUNE 2018) dated 01/07/2019 to carry out this research work.

REFERENCES

[1] V. AMBETHKAR, L.R. BASUMATARY (2021) Heat and mass transfer analysis of combined convection in a horizontal rectangle. *Heat Transfer* **50**(6) 5607-5626.

[2] M. PILLER, E. STALIO (2004) Finite-volume compact schemes on staggered grids. *Journal of Computational Physics* **197**(1) 299-340.

[3] C.H. BRUNEAU, C. JOURON (1990) An efficient scheme for solving steady incompressible Navier-Stokes equations. *Journal of Computational Physics* **89**(2) 389-413.

[4] E. ERTURK, T.C. CORKE, C. GÖKÇÖL (2005) Numerical solutions of 2-d steady incompressible driven cavity flow at high Reynolds numbers. *International journal for Numerical Methods in Fluids* **48**(7) 747-774.

[5] U. GHIA, K.N. GHIA, C. SHIN (1982) High-Re solutions for incompressible flow using the Navier-Stokes equations and a multigrid method. *Journal of Computational Physics* **48**(3) 387-411.

[6] S. SALEM (2006) On the numerical solution of the incompressible Navier-Stokes equations in primitive variables using grid generation techniques. *Mathematical and Computational Applications* **11**(2) 127-136.

[7] M. CORCIONE (2010) Heat transfer features of buoyancy-driven nanofluids inside rectangular enclosures differentially heated at the sidewalls. *International Journal of Thermal Sciences* **49**(9) 153-1546.

[8] I.L. ANIMASAUN, N.A. SHAH, A. WAKIF, B. MAHANTHESH, R. SIVARAJ, O.K. KORÍKO (2002) "Ratio of momentum diffusivity to thermal diffusivity: introduction, meta-analysis, and scrutinization". CRC Press.

[9] G. KUZNETSOV, M. SHEREMET (2006) Two-dimensional problem of natural convection in a rectangular domain with local heating and heat-conducting boundaries of finite thickness. *Fluid Dynamics* **41**(6) 881-890.

[10] J.C. KALITA, D. DALAL, A.K. DASS (2001) Fully compact higher-order computation of steady-state natural convection in a square cavity. *Physical Review E* **64**(6) 066703.

[11] H.K. VERSTEEG, W. MALALASEKERA (2007) "An introduction to computational fluid dynamics: the finite volume method". Pearson education, New Delhi.

[12] S.V. PATANKAR (1980) "Numerical heat transfer and fluid flow". Washington.

[13] H.F. OZTOP, I. DAGTEKIN (2004) Mixed convection in two-sided lid-driven differentially heated square cavity. *International Journal of Heat and Mass Transfer* **47**(8-9) 1761-1769.